Journal of Polymer Research (2021) 28: 397
https://doi.org/10.1007/s10965-021-02769-7

ORIGINAL PAPER

Fluorene substituted thieno[3, 2-*b*]thiophene – a new electrochromic conjugated polymer

Mubashir Shah[1] · Imran Murtaza[1,2] · Rehan Abid[1] · Ahmed Shuja[2] · Hong Meng[3] · Naeem Ahmed[1]

Received: 15 June 2021 / Accepted: 22 September 2021 / Published online: 27 September 2021

Abstract

A new electrochromic conjugated polymer, poly 2-(9,9-dicotyl-9 H-fluorene-2-yl)-3,6-bis(5-hexylthiophen-2-yl)thieno[3,2-*b*]thiophene), containing fluorene (F8-DT6) substituted thieno[3, 2-b]thiophene has been designed by Stille and Suzuki coupling reactions and then polymerized at different potentials through electrochemical polymerization. The as-synthesized polymer is characterized by nuclear magnetic resonance (NMR) spectroscopy, cyclic-voltammetry (CV), ultraviolet-visible spectroscopy (UV-vis), and atomic force microscopy (AFM). The lowest unoccupied molecular orbital (LUMO) and highest occupied molecular orbital (HOMO) energy levels are −2.67 eV and −5.21 eV respectively, as determined by cyclic voltammetry. As the film, P(F8-DT6-TT) exhibits UV-vis at 502 nm, the bandgap values from electrochemical and optical measurements are in excellent agreement. The CIE colour coordinates L^*, a^*, and b^* of neutral and oxidized states are (76.81, −3.04, 67.46) and (68.90, −10.92, 32.04) respectively giving vivid orange colour in the bleached/oxidation state and a very light-yellow colour in the reduced state. P(F8-DT6-TT) exhibits better stability between −0.1 and 2 V and the stability pattern moves towards a stable position by increasing the number of cycles. AFM images reveal a higher root-mean-square value (51.83 nm) that is useful for providing a convenient optical response and film stability. Effective colour tuning by substituting fluorene (F8-DT6) in thieno[3,2-*b*] thiophene units is a notable property of P(F8-DT6-TT), which renders it an appropriate electrochromic material.

Keywords Electrochromism · Redox · Cyclic voltammetry (CV) · Bandgap · Stability · Atomic Force Microscopy (AFM)

Introduction

In recent years, organic electrochromic (OEC) materials have emerged because of their extensive benefits like better coloration performance, smaller absorption band for displaying pure colour, significantly fast-switching speed, and simpler tuning of bandgap with structural modifications as compared with inorganic materials. Electrochromic polymer (ECP) materials are a kind of conjugated polymers that change their optical properties (transmittance, reflectance, and absorbance) with the applied voltage, resulting in a colour shift. If the optical absorptions are in the ultraviolet or infrared region then spectral change due to the redox reactions is visually indistinguishable. Therefore, an electrochromic description may be formulated as colouring or bleaching caused by an electron transfer process when the change is in the visible region. Electrochromic polymers have been utilized in flexible, lightweight, foldable high-performance electronic displays and in fabricating low-cost functional materials. Based on their benefit, they have a wide range of uses, including smart windows, electrochromic fabrics, flexible displays, supercapacitors, sunglasses, and much more [1–9].

The optical memory of an ECP refers to a material's ability to maintain the coloured state after minimizing the applied voltage. In light-emitting diodes (LEDs) and light-emitting electrochemical cells (LECs), it is not always necessary for the displays to be powered to show the colour properties that are desired. In the absence of applied voltage due to the self-erasing mechanism, the solution-based

✉ Imran Murtaza
imran.murtaza@iiu.edu.pk

[1] Department of Physics, International Islamic University, 44000 Islamabad, Pakistan

[2] Centre for Advanced Electronics & Photovoltaic Engineering (CAEPE), International Islamic University, 44000 Islamabad, Pakistan

[3] School of Advanced Materials, Shenzhen Graduate School, Peking University, 518055 Shenzhen, China

electrochromic displays show their coloured/bleached states rapidly. Whereas the π-conjugated polymers are well attached to electrodes due to which the self-erasing effect is minimized. The electrochromic switching rate depends on the time required by the electro chrome to convert from one redox state to another. It relies on few conditions, like the ion transferability and the diffusion of these species in the active layer of ECP. The optical change will also be affected by the morphology and thickness of the deposited EC layer [10–12]. Different colours have been obtained by the designing and modification of substituted backbone structures, such as poly(*p*-phenylenevinylene) (PPV) and polyfluorene (PF), to achieve full-colour display [13]. In Thieno[3,2-*b*]thiophene (TT), the fused TT part has a greater degree of conjugation to provide polymers with a smaller bandgap and better charge transport property in contrast with thiophene. So, it is considered to be an important molecule in the organic electronic field [14]. In solid-state organic materials such as organic photovoltaics (OPVs), a unit of thieno[3, 2-*b*]thiophene has a rigid configuration and an expanded π-conjugation which is suitable for modifying the bandgap with enhancing intermolecular interactions [15–17].

In this paper, we present the synthesis of F8-DT6-TT through palladium-catalyzed Stille and Suzuki coupling reactions and investigate its electrochromic aspects through electrochemical polymerization. The as-synthesized polymer shows enhanced redox-dependent electrochromic properties which were analysed by cyclic-voltammetry, ultraviolet-visible spectroscopy, and atomic force microscopy. Fluorene substituted thieno[3,2-*b*] thiophene conjugated polymer initiates distinctions in electrochemical, optical, and morphological behaviours. Therefore, for electrochromic materials, substitution is possibly a sharp tuning method.

Experimental details

Chemicals

All of the initial supplies were ordered from Energy Chemical, but palladium catalyst $Pd(PPh_3)_4$ was purchased from TCl. Dichloromethane (DCM) and chloroform ($CHCl_3$) were processed and filtered in a nitrogen atmosphere over calcium hydride. Acetic acid, tetrabromo-thienothiophene, zinc powder, 3,6dibromothieno[3,2-*b*]thiophene, tributyl(5-hexylthiophen-2-yl)stannane, anhydrous toluenemethanol, N-Bromosuccinimide, chloroform, acetic acid, sodium bicarbonate ($NaHCO_3$), dichloromethane, magnesium sulphate ($MgSO_4$), 2,5-dibromo-3,6-bis(5-hexylthiophen-2yl)thieno[3,2-b]thiophene,2,2'-(9,9-dioctyl-9 H-fluorene2,7diyl) bis(4,4,5,5-tetramethyl-1,3,2-dioxaborolane), toluene, potassium carbonate, aliquat$_{336}$, acetone and hexane were used to synthesize compound 2-(9,9-dicotyl-9 H-fluorene-2-yl)-3,6-bis(5-hexylthiophen-2-yl)thieno[3,2- *b*]thiophene).

Synthesis

Scheme 1 demonstrates a synthesis approach for the preparation of F8-DT6-TT. At first, to design 3,6-dibromothieno[3,2-b]thiophene (3), acetic acid (100 cm^3) was dissolved in tetrabromo-thienothiophene (1.0 g, 2.20 mmol) then agitated in a vessel attached to a condenser in such a way that vapours condensed continuously (reflux heating) and then added zinc powder (0.15 g, 2.30×10^{-3} mol) to the solution. This solution was again agitated under reflux for 30 min. After cooling more zinc powder (0.15 g, 2.30×10^{-3} mol) was added to the mixture and continued refluxing for further 30 min. Water was added to the mixture to dilute it then filtered, desiccated, cooled to room temperature, and purified by column chromatography over silica gel (CH_2Cl_2 :petroleum = 3:1). Light petroleum eluted 3, 6- dibromo-thieno[3, 2-*b*]thiophene (0.50 g, 76 %), mp 120–122 °C (from light petroleum); ν_{max} / cm^{-1} 727 (C-Br); δH 7.32 (2 H, s, H-2/5) (Found: H, 0.8 %; C, 24.6; M^++1 296.8050. $C_6H_2Br_2S_2$ requires H, 0.7 %; C, 24.2; M + 1, 296.8044). The other intermediate compound (5) tributyl(5-hexylthiophen-2-yl)stannane was prepared by a known literature procedure [18].

Now to synthesize the compound 3,6-bis(5-hexylthiophene-2-yl)thieno[3,2-b]thiophene (6), 3,6-dibromothieno[3,2-*b*]thiophene (5 mmol, 1.48 g), tributyl(5-hexylthiophen-2-yl)stannane (18.75 mmol, 8.87 g) and anhydrous toluene (100 mL) were added in 300 mL Schlenk flask. The mixture of solution was purged with nitrogen for 30 min. After that, the reaction mixture was heated to 105 °C with the addition of $Pd(PPh_3)_4$ in one portion and then kept at this temperature for 12 h over stirring. Then, the mixture was left to cool down and poured into methanol. The grey precipitate was washed off and then cleaned with water and methanol. The precipitate was refined through column chromatography over silica gel (CH_2Cl_2 :petroleum = 3:1) to yield 3,6-bis(5-hexylthiophene-2yl)thieno[3,2-b]thiophene (6) (1.2 g, 50 % yield): ^{1}H NMR (400 MHz, $CDCl_3$) δ 7.44 (s, 2 H), 7.20 (*d, J* = 3.5 Hz, 2 H), 6.78 (*d, J* = 3.5 Hz, 2 H), 2.84 (*t, J* = 7.6 Hz, 4 H), 1.72 (*dt, J* = 15.3, 7.5 Hz, 4 H), 1.62 (*dt*, 6.9 Hz, 2 H, *J* = 8.5), 1.36–1.31 (m, 10 H), 0.90 (m, 6 H).

For the synthesis of 2,5-dibromo-3,6-bis(5-hexyl thiophene-2-yl)thieno[3,2-b]thiophene (7): N-Bromosuccinimide (0.15 g, 0.84 mmol) was added in a solution of compound 6 (0.2 g, 0.42 mmol) in $CHCl_3$ (3 ml) and HOAc (3 ml) at -20 °C. The mixture was stirred overnight and warmed slowly to room temperature. This solution was transferred to saturated aqueous $NaHCO_3$ and drawn out with DCM (50 mL). The organic phase

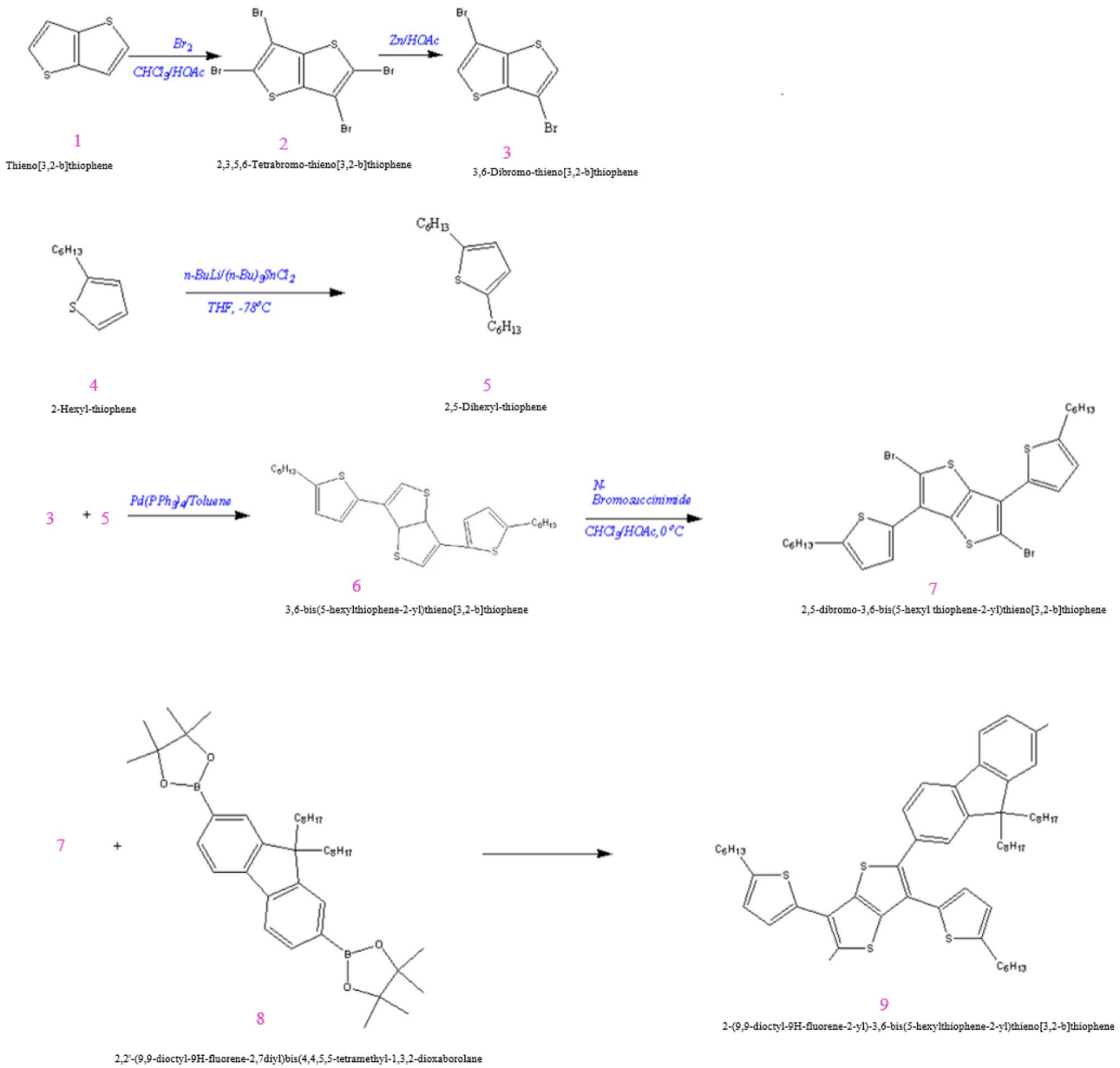

Scheme 1 Synthetic route to F8-DT6-TT

was dehydrated over $MgSO_4$. Under rotating evaporation, the solvent was dispersed to obtain the unrefined yield which was then purified through column chromatography (CH_2Cl_2 /hexane, 1:1). Yield: 50 %.[1] H NMR ($CDCl_3$, 300 MHz) δ 7.39 (*d, 2 H, J* = 3.6 Hz), 6.84 (*d, 2 H, J* = 3.6 Hz), 2.86 (*t, 4 H, J* = 7.7 Hz), 1.80–1.67 (m, 4 H), 1.42–1.25 (m, 12 H), 0.91 (*t, 6 H, J* = 6.9 Hz). At the end, for the preparation of compound 9: 2,5-dibromo-3,6-bis(5-hexyl thiophene-2-yl)thieno[3,2-b]thiophene (7) (1.0 g, 1.59 mmol), 2,2'-(9,9-dioctyl-9 H-fluorene-2,7diyl) bis(4,4,5,5-tetramethyl-1,3,2-dioxaborolane) (8) (1.02, 1.59 mmol), 8 mL toluene, 2 M potassium carbonate (3.18 mL) and aliquat$_{336}$ (0.64 g, 1.59 mmol) were added in a 25 ml Schlenk flask. By purging with nitrogen for 30 min, $Pd(PPh_3)_4$ (0.037 g, 0.0318 mmol) was included in one part and heated at 105 °C. The mixture was maintained at this temperature for 3 days under stirring. After being cooled down, the reaction mixture was transferred to methanol. Through Soxhlet extraction, the unrefined product was then purified, with MeOH, hexane, acetone, and $CHCl_3$, sequentially. The $CHCl_3$ fraction was concentrated and precipitated in MeOH. The desired product was filtered off and dried under the vacuum. [1] H NMR (300 MHz, $CDCl_3$) δ 7.72 (*d, J* = 8.1 Hz, 10 H), 7.51 (*d, J* = 7.1 Hz, 6 H), 7.44

(s, 10 H), 6.95 (*d, J* = 3.4 Hz, 6 H), 6.66 (*d, J* = 3.1 Hz, 4 H), 2.78 (*t, J* = 7.4 Hz, 4 H), 1.66–0.85 (m, 20 H).

F8-DT6-TT was synthesized via Stille and Suzuki reactions. To verify the successful formation of chemical, NMR spectroscopy was done. After that, electrochemical polymerization was done through an electrochemical workstation. The thickness of the laminated films on the indium tin oxide (ITO) glass was calculated using a Bruker DEKTAK XT Profilometer. AFM (Atomic Force Microscope) was used to examine the morphology of the polymer's film.

Results and discussion

Cyclic-voltammetry

The polymerization and electrochemical tests were carried out in a three-electrode compartment with ITO coated glass, silver and platinum as working, pseudo reference and counter electrodes, respectively. Through oxidative electro-polymerization, thin film of the polymer was deposited on ITO coated glass substrate in dichloromethane (DCM) solution containing 0.1 M tetra-butyl-ammonium hexa-fluoro- phosphate ($TBAPF_6$) and 0.69×10^{-3} M monomer. Potential window ranging from −0.1 to 2.0 V was scanned at a speed of 100 mVs^{-1} for 10 cycles as shown in Fig. 1. During electrochemical polymerization, monomer has been polymerized significantly to produce highly electroactive polymer. In the 1st cycle of CV, irreversible oxidation peak is produced. With increasing current intensity, new reversible redox pairs are noticed which confirm that the electroactive polymer film has been successfully deposited on the ITO surface. The peak values of anodic ($I_{p.a.}$) and cathodic (I_{pc}) currents after 10 cycles are 0.44 and −0.63 A respectively.

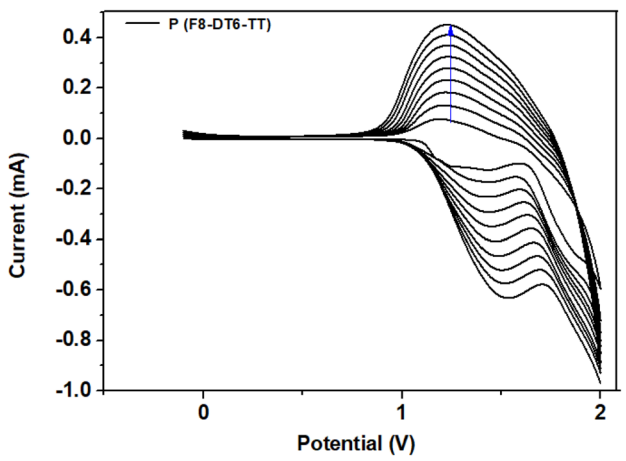

Fig. 1 Electrochemical polymerization of P(F8-DT6-TT). The potentials are scanned between −0.1 and 2.0 V at a scan rate of 100 mV s^{-1} for 10 cycles

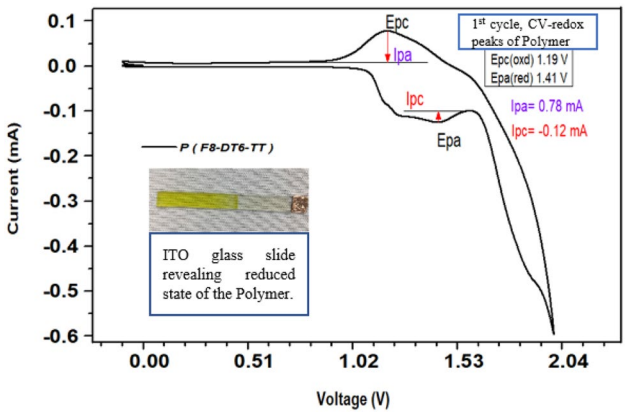

Fig. 2 Cyclic voltammetry of P(F8-DT6-TT) thin film with a thickness of 150 nm on ITO coated glass substrate

Figure 2 shows the cyclic voltammetry of P(F8-DT6-TT) thin film with a thickness of 150 nm on ITO coated glass substrate. In the CV curve, the first oxidation peak is recorded at 1.19 V and first reduction peak is observed at 1.41 V due to the generation of charge carriers. If the applied potential is increased, the polaronic and bipolaronic bands expand more and more. For the colour identification of synthesized polymer, CIE colour coordinates L^*, a^*, and b^* were measured. $L^*a^*b^*$ describes the variations in colour transfer of electrochromic polymers as a function of applied voltage. [19]. The relative (L^*; a^*; b^*) values of neutral and oxidized states for polymer P(F8-DT6-TT) are (76.81, −3.04, 67.46) and (68.90, −10.92, 32.04) respectively, giving vivid orange colour in oxidized state and very light-yellow colour in the reduced state as shown in Fig. 3.

The outcomes of electrochemical polymerization are outlined in Table 1. Based on the onset oxidation peaks and the ferrocene/ ferrocenium reference redox potentials (Fc/Fc^+ vs. the pseudo-reference electrode of silver wire, 0.52 V), the LUMO and HOMO levels values are −2.67 and −5.21 eV respectively for P(F8-DT6-TT) polymer. The optical bandgap ($E_{g,opt}$) is correlated with the wavelength of 502 nm.

UV-visible spectroscopy

Optical studies of the conducting polymers are useful in formulating the defect states which govern their other properties such as electronic transport. In-situ spectroelectrochemical (SEC) calculations were carried out with UV-Vis-NIR spectrophotometer containing a potentiostat/galvanostat in a monomer free ACN solution carrying 0.1 M $TBAPF_6$ to study optical properties at different applied potentials. In Fig. 4, SEC measurements of 150 nm P(F8-DT6-TT) thin film on the ITO-coated glass are shown. The inset corresponds to –0.1 V which illustrates the measurement of the optical bandgap from Tauc plot.

Fig. 3 Colour variations in oxidized and non-oxidized state

In a fully reduced state of P(F8-DT6-TT) at –0.1 V, two absorption bands appear in the visible region (480 and 445 nm) due to the development of a more rigid and well-organized polymer backbone. By applying low voltage of + 1 V, maximum absorption wavelength appears at 476 nm. In the fully oxidized state at 2.0 V, the polymer shows low absorption in the visible region. On oxidation, the intensity of absorption peaks decreases at 480 nm. However, some new broad bands of absorption have been observed at 600 and 655 nm as a result of charge carrier generation (polarons and bipolarons) following the above-mentioned CV data. The optical energy bandgap of 2.47 eV corresponding to the wavelength of 502 nm has been calculated.

Stability

For device applications e.g., electrochromic and optical, the fast-switching time is favourable and the cycle lifetime is a significant parameter. The deposited thin film reveals porous, rough morphology and high electro-activity for ion penetration and show a fast-switching speed. It can be seen in Fig. 5, that the transmission value varies from highest to lowest at the same wavelength as the polymer is reduced from an oxidized state, here it is noted that the transmittance has been measured in the visible region where the best value of optical contrast is observed. To detect the change in percentage transmittance (ΔT%) of polymer between reduced and oxidized states, the maximum optical contrast at a stepping potential of –0.1 to 0.4 V is determined. Now during reduction state transmittance of the thin film is 27% and in oxidation state transmittance is 57%, therefore the calculated value of optical contrast is ΔT%= 30% and overall performance seems to be stable up to 30 cycles.

To study the stability of the polymer, P(F8-DT6-TT) film was cycled 50 times from − 0.1 to + 2.0 V as shown in Fig. 6. The peak anodic current is recorded on 10th, 20th, 30th, 40th and 50th cycle, with increasing number of cycles, there is no marked variation in peak anodic current ($I_{p.a.}$) that demonstrates the successful deposition and growth of polymer film on ITO substrate (working electrode) and also indicates systematic growth of electrode area due to deposition of P(F8-DT6-TT) film. Similarly, for peak cathodic current (I_{pc}), there is marked decrease in I_{pc} on 20th cycle towards the negative current value that exhibits the irreversible nature of cathodic reduction process of deposited P(F8-DT6-TT) film. Then after 20th cycle I_{pc} rises and remains constant on 30th, 40th, and 50th cycles

Table 1 Optical and electrochemical properties of the P(F8-DT6-TT) polymer

Polymer	E_{ox} onset	E_{red} *onset*	$E_{p,ox}$	$E_{p.red}$	E_{HOMO}[a]	E_{LUMO}[b]	$E_{g(CV\ Scan)}$	$E_{g,opt}$[c]
	(V)	(V)	(V)	(V)	(eV)	(eV)	(eV)	(eV)
F8-DT6-TT	0.93	–1.61	1.19	1.41	–5.21	–2.67	2.54	2.47

[a] E_{HOMO}= -[(E_{ox}onset - $E_{1/2(ferrocene)}$) + 4.8] eV

[b] E_{LUMO} = -[(E_{red}onset - $E_{1/2(ferrocene)}$) + 4.8] eV

[c] $E_{g,opt}$ calculated from absorption edge shown in Fig. 4, at voltage of –0.1 V [20, 21]

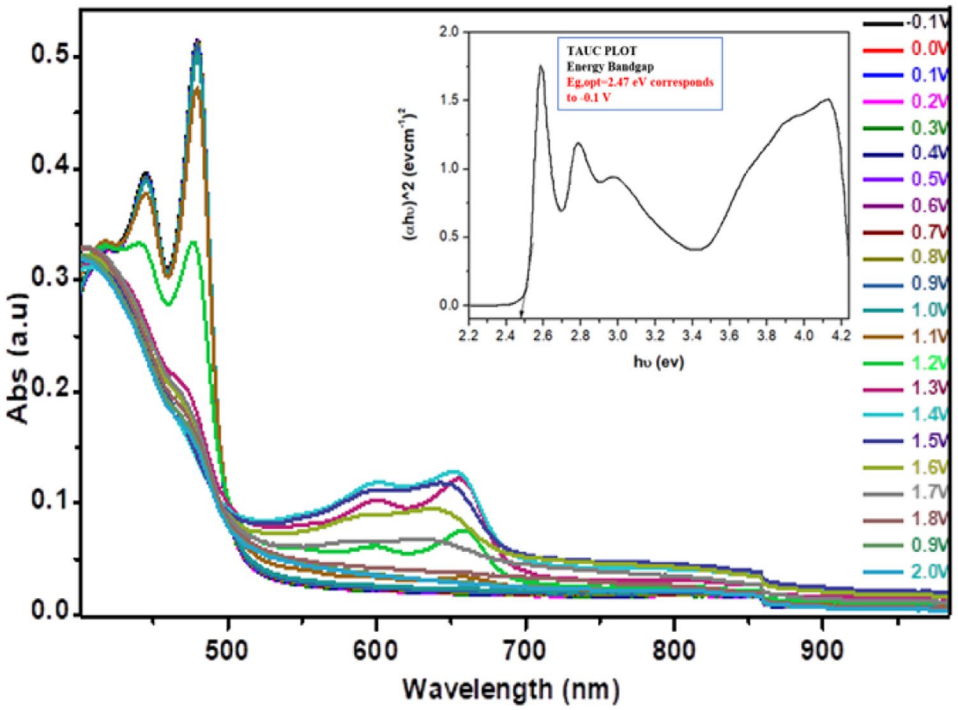

Fig. 4 Spectroelectrochemistry (SEC) of 150 nm P(F8-DT6-TT) film on the ITO-coated glass slide in 0.1 M $TBAPF_6$ solution at the applied potential range of –0.1 V to + 2.0 V (inset: Tauc plot at -0.1 V for determining the optical bandgap)

that shows reversible nature of cathodic reduction process. Furthermore, the stability pattern moves towards a stable position by increasing the number of cycles.

Atomic force microscopy

AFM images are shown in Fig. 7. Generally, by increasing the roughness and porosity of the film the ions freely move across the film to promote the redox process of the film. To get the morphology of the thin film surface, the AFM of electrochemically deposited polymer on an ITO film was performed. As shown in Fig. 7, a quite flat and homogeneous morphology has been observed and the root-mean-square (RMS) surface roughness value for the film is 51.83 nm. This morphology is useful for device applications because counter ions can quickly pass into polymers

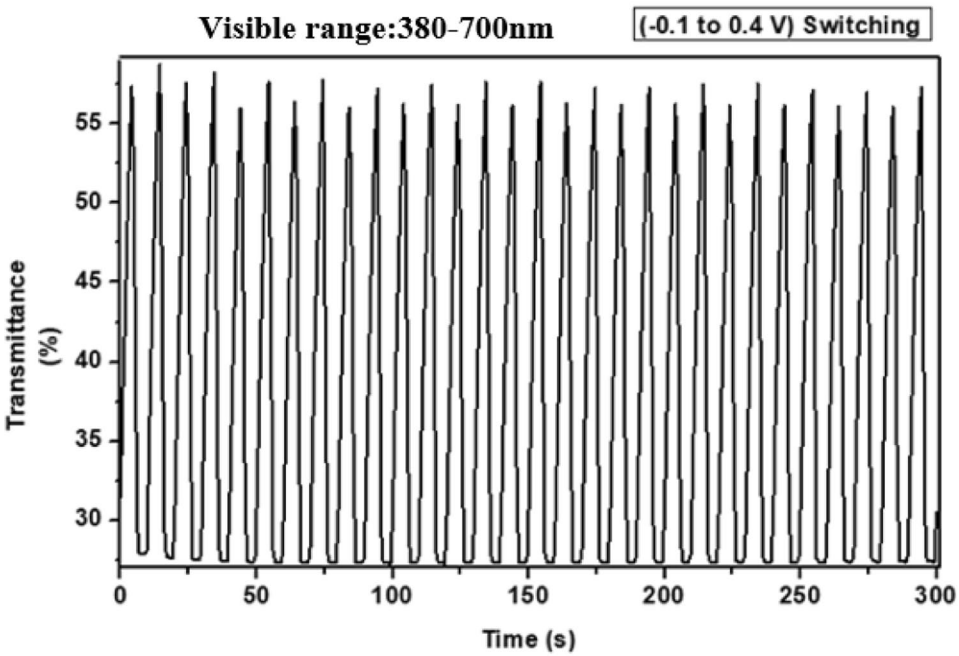

Fig. 5 The transmittance of P(F8-DT6-TT) at a stepping potential between − 0.1 to 0.4 V with a switching interval of 10 s

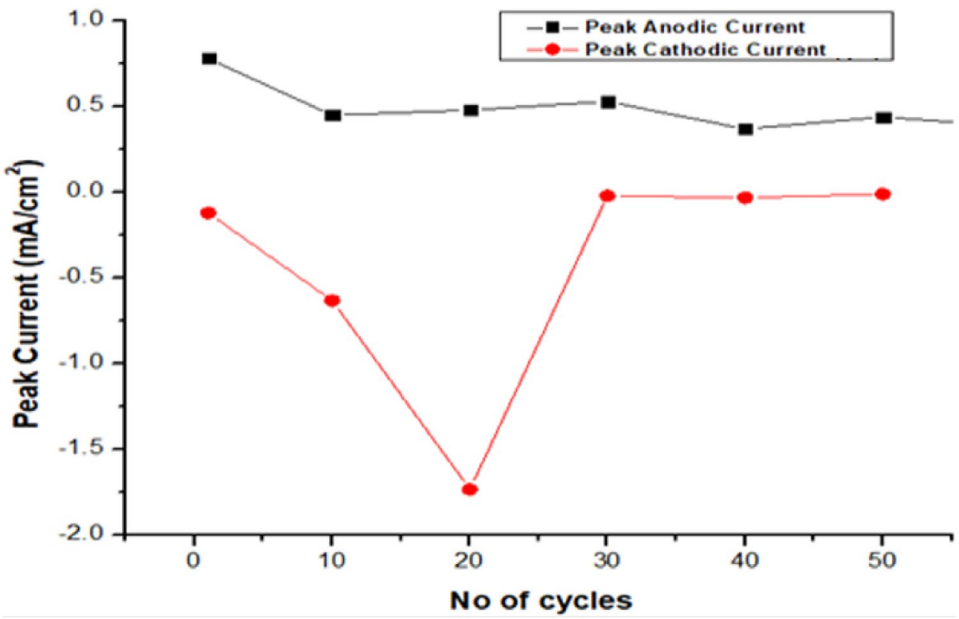

Fig. 6 Stability of P(F8-DT6-TT) film cycled 50 times with a scan rate of 100 mV s^{-1}, in 0.1 M $TBAF_6$/AC

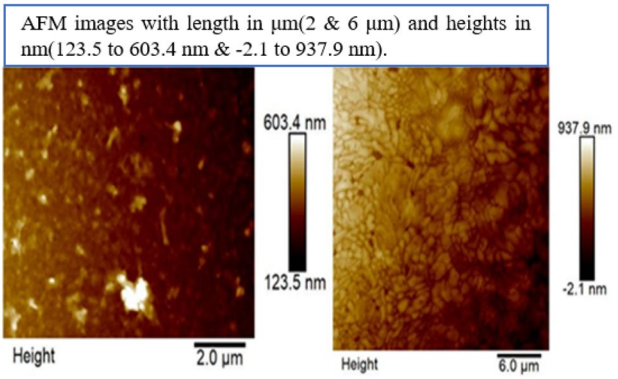

Fig. 7 AFM (Atomic Force Microscopy) of P(F8-DT6-TT), the root-mean-square (RMS) surface roughness values obtained of 51.83 nm for the film

film which increases redox stability [22]. The higher R_{RMS} is convenient for doping/de-doping process which gives a better optical response and film stability.

P(F8-DT6-TT) shows higher E_{ox} onset which may demonstrates less electro-rich nature of fluorine in thieno[3,2-b]thiophene core, that may significantly stabilize the positive carriers in oxidation process. The lowest *λonset* reveals higher conductivity, that is attributed to electrical conducting property of the thieno[3,2-b]thiophene unit. The increase in optical energy gap of polymer P(F8-DT6-TT) is due to the fluorine substituted thieno[3,2-b]thiophene because thieno[3,2-b]thiophene units increase polymer coplanarity or creates new delocalized HOMO pattern over the backbone, that we anticipate will improve intermolecular charge-carrier leaping. Moreover, P(F8-DT6-TT) shows significantly high colour efficiency in the visible region at the maxima of their optical absorption (502 nm). Therefore, for electrochromic materials substitution is sharp tuning method because this may extend the set of available colours that is suitable for full colour displays.

Polymer	E_{ox} onset (V)	E_{HOMO} (eV)	*λonset* (nm)	$E_{g,opt}$ (eV)	Neutral state $L^*/a^*/b^*$	Oxidized state $L^*/a^*/b^*$	Ref.
P(F8-DT6-TT)	0.93	–5.21	502	2.47	76.81/-3.04/67.46 (Light yellow colour)	68.90/ -10.92/ 32.04 (Vivid orange colour)	This work
P(CNPh-ETTE)	0.09	–4.37	688	1.54	35.7/4.4/-2.5 (Purple)	44.1/-2.4/4.1 (Pale grey-blue)	[14]
P(Py-ETTE)	0.83	–5.11	698	1.72	39.6/1.5/-1.4 (Sand brown)	48.4/3.1/8.9 (Pale grey green)	[14]
P(Ph-ETTE)	0.07	–4.35	731	1.80	30.5/3.9/-8.9 (Deep blue)	33.9/-4.0/-13.5 (Transparent)	[14]

Conclusions

In summary, the synthesis and characterization of novel electrochromic conjugated polymer, fluorene substituted thieno[3,2-*b*] thiophene, has been demonstrated. Conducting polymer P(F8-DT6-TT) provides vivid orange color in the bleached/oxidized state and the reduced state gives a very light-yellow color, good bandgap value ($E_{g,opt}$ 2.47 eV), and higher R_{RMS} (51.83 nm), which gives a better optical response and film stability. From these outcomes, it can be concluded that fluorene (F8-DT6) substituted thieno[3,2-*b*] thiophene conjugated polymer is an appropriate unit in electrochromic polymers, and excellent colour tuning can be attained in thieno[3, 2-*b*]thiophene by substituting fluorene which is confirmed by the analysis of electrochemical, optical and morphological behaviours. In consequence, this can extend the collection of available colours that is appropriate for colour displays. Hence, for electrochromic materials substitution is possibly a sharp tuning method.

Funding This work was financially supported by the Pakistan Science Foundation under the provision of Pakistan Science Foundation-National Natural Science Foundation of China grant (PSF/NSFC-II/ENG/C-IIUI-06).

Declarations

Author statement It is stated that all authors are aware of the manuscript submission and they have no conflict of interest.

Conflict of interest The authors declare no conflicts of interest.

References

1. Zhang Z, Rouabhia M, Moulton SE (eds) (2018) Conductive Polymers: Electrical Interactions in Cell Biology and Medicine. CRC Press, London
2. Zhang L, Du W, Nautiyal A, Liu Z, Zhang X (2018) Recent progress on nanostructured conducting polymers and composites: synthesis, application and future aspects. Sci China Mater 61:303–352
3. Reynolds JR, Thompson BC, Skotheim TA (eds) (2019) Conjugated Polymers: Properties, Processing, and Applications. CRC press, London
4. Vu TD, Liu S, Zeng X, Li C, Long Y (2020) High-power impulse magnetron sputtering deposition of high crystallinity vanadium dioxide for thermochromic smart windows applications. Ceram Int 46:8145–8153
5. Li K, Zhang Q, Wang H, Li Y (2014) Red, green, blue (RGB) electrochromic fibers for the new smart color change fabrics. ACS Appl Mater Interfaces 6:13043–13050
6. Cai G, Darmawan P, Cui M, Wang J, Chen J, Magdassi S, Lee PS (2016) Highly stable transparent conductive silver grid/PEDOT: PSS electrodes for integrated bifunctional flexible electrochromic supercapacitors. Adv Energy Mater 6:1501882
7. Österholm AM, Shen DE, Kerszulis JA, Bulloch RH, Kuepfert M, Dyer AL, Reynolds JR (2015) Four shades of brown: tuning of electrochromic polymer blends toward high-contrast eyewear. ACS Appl Mater Interfaces 7:1413–1421
8. Mortimer RJ, Dyer AL, Reynolds JR (2006) Electrochromic organic and polymeric materials for display applications. Displays 27:2–18
9. Runnerstrom EL, Llordés A, Lounis SD, Milliron DJ (2014) Nanostructured electrochromic smart windows: traditional materials and NIR-selective plasmonic nanocrystals. Chem Commun 50:10555–10572
10. Yu H, Shao S, Yan L, Meng H, He Y, Yao C, Xu P, Zhang X, Hu W, Huang W (2016) Side-chain engineering of green color electrochromic polymer materials: toward adaptive camouflage application. J Mater Chem C 4:2269–2273
11. Li W, Guo Y, Shi J, Yu H, Meng H (2016) Solution-processable neutral green electrochromic polymer containing thieno [3, 2-b] thiophene derivative as unconventional donor units. Macromolecules 49:7211–7219
12. Brooke R, Mitraka E, Sardar S, Sandberg M, Sawatdee A, Berggren M, Crispin X, Jonsson MP (2017) Infrared electrochromic conducting polymer devices. J Mater Chem C 5:5824–5830
13. Tang W, Ke L, Tan L, Lin T, Kietzke T, Chen ZK (2007) Conjugated copolymers based on fluorene – thieno [3, 2-b] thiophene for light-emitting diodes and photovoltaic cells. Macromolecules 40:6164–6171
14. Shao S, Shi J, Murtaza I, Xu P, He Y, Ghosh S, Zhu X, Perepichka IF, Meng H (2017) Exploring the electrochromic properties of poly (thieno [3, 2-b] thiophene) s decorated with electron-deficient side groups. Polym Chem 8:769–784
15. Xu P, Murtaza I, Shi J, Zhu M, He Y, Yu H, Goto O, Meng H (2016) Highly transmissive blue electrochromic polymers based on thieno [3, 2-b] thiophene. Polym Chem 7:5351–5356
16. Xu SJ, Zhou Z, Liu W, Zhang Z, Liu F, Yan H, Zhu X (2017) A Twisted Thieno [3, 4-b] thiophene-Based Electron Acceptor Featuring a 14-π-Electron Indenoindene Core for High-Performance Organic Photovoltaics. Adv Mater 29:1704510
17. Za'aba NK, Taylor DM (2019) Photo-induced effects in organic thin film transistors based on dinaphtho [2, 3-b: 2′, 3′-f] Thieno [3, 2-b′] thiophene (DNTT). Org Electron 65:39–48
18. Pan Z, Liu Y, Fan F, Chen Y, Li Y, Zhan X, Song Y (2013) Self-Assembled π-Extended Condensed Benzothiophene Nanoribbons for Field-Effect Transistors. Chem Eur J 19:9771–9774
19. Shi J, Zhu X, Xu P, Zhu M, Guo Y, He Y, Hu Z, Murtaza I, Yu H, Yan L, Goto O (2016) A Redox-Dependent Electrochromic Material: Tetri-EDOT Substituted Thieno [3, 2-b] thiophene. Macromol Rapid Commun 37:1344–1351
20. Costa JC, Taveira RJ, Lima CF, Mendes A, Santos LM (2016) Optical band gaps of organic semiconductor materials. Opt Mater 58:51–60
21. Pakkath R, Reddy EK, Kuriakose S, Saritha C, Sajith AM, Karuvalam RP, Haridas KR (2019) Synthesis, characterization and determination of HOMO-LUMO of the substituted 1, 3, 5-triazine molecule for the applications of organic electronics. J Korean Chem Soc 63:352–359
22. Zhao H, Wei Y, Zhao J, Wang M (2014) Three donor-acceptor polymeric electrochromic materials employing 2, 3-bis (4-(decyloxy) phenyl) pyrido [4, 3-b] pyrazine as acceptor unit and thiophene derivatives as donor units. Electrochim Acta 146:231–241